富山大学水素同位体機能研究センター研究報告18：105－116，1998.

論文

焼結法により作成したMg_2Ni電極の充放電特性に及ぼす酸化の影響

波多野雄治[1]、小林幸司[2]、森　克徳[2]、渡辺国昭[1]、諸住正太郎[1]

[1]富山大学水素同位体機能研究センター
[2]富山大学工学部物質生命システム工学科
〒930-8555　富山市五福3190番地

Influence of Pre-oxidation on Charge/Discharge Characteristics of Sintered Mg_2Ni

Yuji HATANO[1], Koji KOBAYASHI[2], Katsunori MORI[2], Kuniaki WATANABE[1] and Shotaro MOROZUMI[1]

[1]Hydrogen Isotope Research Center,
[2]Material Systems Engineering and Life Science, Faculty of Engineering,
Toyama University, Gofuku 3190, Toyama 930-8555, Japan

(Received January 19, 1999; accepted March 15, 1999)

Abstract

The influence of pre-oxidation on charge/discharge characteristics of sintered Mg_2Ni electrodes was examined with an open electrochemical cell. Mg_2Ni powder was first oxidized slightly in air at 473 K for 5-360 min and then sintered in argon atmosphere at 823 K. The cyclic stability of discharge capacity was improved markedly by pre-oxidation. Maximum cycle life was obtained using 20 min pre-oxidation. The mechanism by which pre-oxidation influences cyclic stability was examined via density measurement and surface analysis. The sintering rate had a maximum value for 20 min pre-oxidation. An MgO layer was formed on the surface of Mg_2Ni during sintering and growth rate of the MgO layer decreased with pre-oxidation. Improvement of cyclic stability with pre-oxidation was attributed to the firm aggregation between Mg_2Ni powder particles due to reduction in the thickness of MgO layer.

1. Introduction

Magnesium-based alloys are recognized as promising materials for the electrodes of nickel/metal hydride batteries because of their high hydrogen absorption capacity. In fact, it has been reported that the discharge capacity of amorphous Mg-Ni based alloys prepared by mechanical alloying was higher than theoretical discharge capacities of conventional hydrogen storage materials such as AB_5 and AB_2 type alloys in the initial stage of charge/discharge cycles[1-5]. The cyclic stability of discharge capacity of these alloys, however, was poor, i.e. the discharge capacity decreases rapidly with increasing charge/discharge cycles[1-5]. Therefore, it is important to clarify the degradation mechanism of Mg-Ni based alloys.

The present authors have recently examined the charge/discharge characteristics of Mg_2Ni electrodes prepared by sintering without any binder. The advantage of this preparation technique is that the electrochemical properties of the material can be evaluated without any influence of a binder. It has been reported in our previous paper that the degradation rate of Mg_2Ni electrode is sensitively dependent on sintering temperature[6]. The effect of sintering temperature was ascribed to the pore structure of Mg_2Ni powder constituting the electrodes, the aggregation states of powder particles, and their chemical surface states. The mechanism of degradation, however, was not fully clarified.

The pore structure and the aggregation states would vary with the surface treatment before the sintering as well as the chemical surface states since the sintering rate would be influenced sensitively by impurity layers on the particle surfaces. Therefore, it is important to investigate the influence of surface treatment on the cyclic stability for clarification of the degradation mechanism. In the present paper, the influence of pre-oxidation on the degradation behavior of sintered Mg_2Ni electrodes is examined. The influence of pre-oxidation on the sintering rate is evaluated by measuring the density of sintered material, and the influence on the chemical surface state is investigated with X-ray photoelectron spectroscopy (XPS). The relation of degradation rate with the aggregation states of powder and the chemical surface state is discussed.

2. Experimental

To prepare the sample anode, the Mg_2Ni powder of 0.5 g was first oxidized in air at 473 K for 5-360 min and then cold pressed onto a nickel mesh with 40 MPa into a sheet of 15 $\times$ 20 $\times$ 1 mm. It was then sintered at 823 K for 90 min in flowing argon at 0.1 MPa. The schematic description of the electrode is shown in Fig. 1. Another type of specimen was also

prepared from powder as-received, i.e. the powder without the pre-oxidation, for comparison, where the similar procedures were applied for the anode preparation except for the pre-oxidation.

The charge/discharge cycle test was carried out with a conventional open cell filled with two electrodes and 6 M KOH aqueous solution, where $NiOOH/Ni(OH)_2$ was used as the cathode material. The charge/discharge cycle consisted of three steps: charging step at 40 mA for 30 min, rest step for 5 min and discharge step at 10 mA to 1 V.

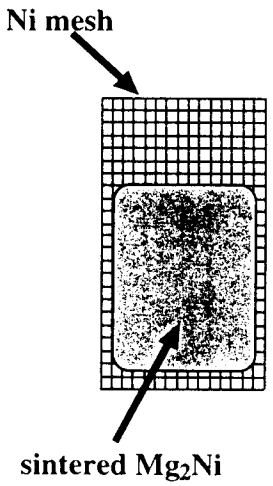

Fig. 1 Schematic description of sintered Mg_2Ni electrode.

In the case of the density measurement, 0.2 g of powder was cold pressed into a disk (9 mm in diameter, 1 mm in thickness) and then sintered in the manner described above. The mass of sintered disk was measured with a microbalance, and its volume was estimated by measuring the buoyancy in water with the microbalancce. The uncertainty of density was 0.1 $g \cdot cm^{-3}$.

The variation of chemical surface state of Mg_2Ni during the pre-oxidation and the sintering was examined with XPS. Here, Mg_2Ni sheets (5 × 10 × 1 mm) prepared by melting were used instead of the sintered material. The surfaces were first polished with abrasive papers. Three kinds of specimen were then prepared with the following treatments: (1) oxidation in air at 473 K for 20 min, (2) oxidation in air at 473 K for 20 min plus heating in argon atmosphere at 823 K for 90 min, (3) heating in argon atmosphere at 823 K for 90 min. These conditions of oxidation in air and heating in argon are the same as those in the pre-oxidation and the sintering. The XPS analysis was carried out in a ultra high vacuum chamber whose base pressure was 1 × 10^{-7} Pa. Non-monochromatized Mg K_α radiation (1253.6 eV) was used for the photoelectron excitation.

3. Results and discussion

3.1. Discharge characteristics

The influence of pre-oxidation on the discharge characteristics is shown in Fig. 2. In the initial stage of charge/discharge cycles, the discharge capacity increased rapidly and reached to the maximum value, 40-50 $mA \cdot h \cdot g^{-1}$, within 3 cycles. Here the variation in the maximum values is due to different specimen masses brought about by peeling of the powder

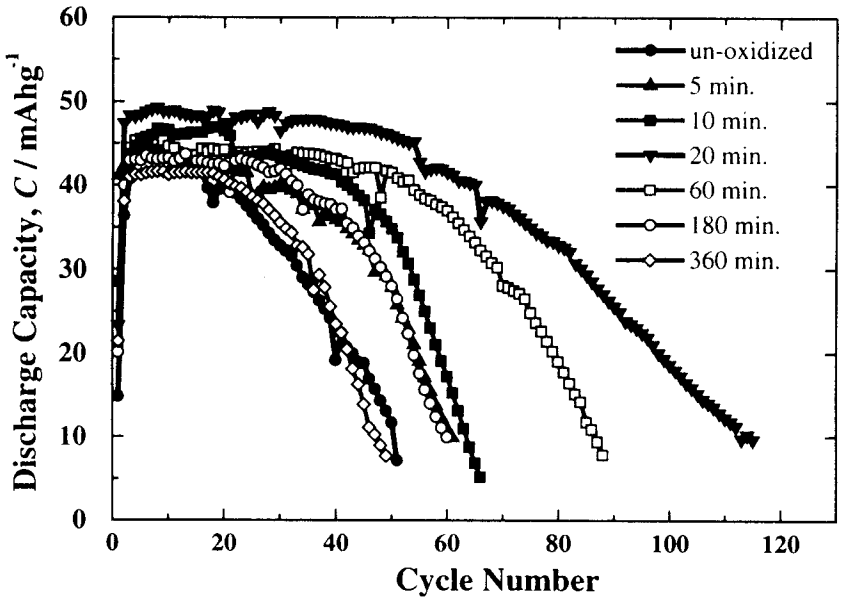

Fig. 2 Influence of pre-oxidation on discharge characteristics.

particles during the preparation. Then, the discharge capacity maintained almost constant value for 20-60 cycles, and decreased gradually. It should be noted that the un-oxidized specimen was degraded in the discharge capacity in advance of the pre-oxidized specimens, and that the degradation rate, i.e. the decrease of discharge capacity per cycle, was higher for the former than for the latter. That is the cyclic stability of discharge capacity was improved by the pre-oxidation. Cycle life is defined here as the cycle number at which the discharge capacity decreased to a half of the maximum value. The variation of cycle life with the oxidation time is shown in Fig. 3, in which the cycle life of the un-oxidized specimen is also plotted for comparison. The cycle life of the pre-oxidized specimen first increased with the oxidation time, had the maximum value at 20 min, and then decreased gradually. The

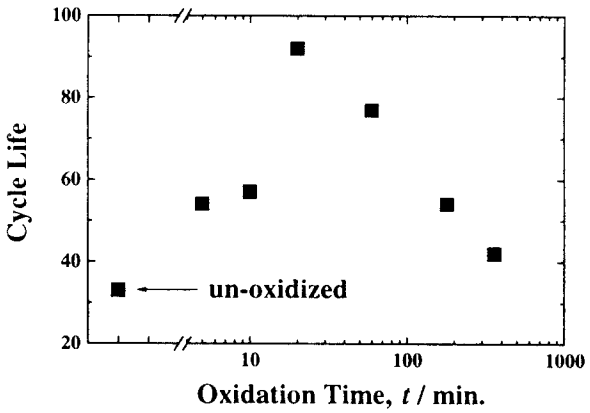

Fig. 3 Influence of pre-oxidation on cycle life.

cycle life of the specimen oxidized for 20 min was 3 times longer than that of the un-oxidized specimen.

The potential variation of pre-oxidized specimen (20 min) during the discharge at 15th cycle is shown in Fig. 4 together with that of the un-oxidized specimen. The potential is lower for the pre-oxidized specimen than for the un-oxidized one. That is the difference between the measured potential and the theoretical discharge voltage (1.318 V) which is called as overpotential was higher for the former than for the latter. The mechanism of this difference in the overpotential is discussed in 3.4.

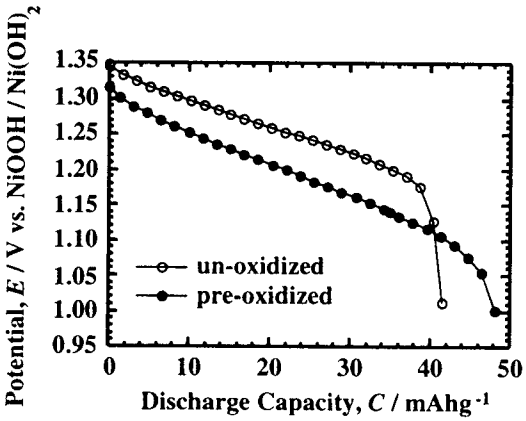

Fig. 4 Potential variation of pre-oxidized and un-oxidized specimens during discharge at 15th cycle.

3.2. Influence of pre-oxidation on sintering rate

The influence of pre-oxidation on the density of sintered Mg_2Ni is shown in Fig. 5. The density of the pre-oxidized specimens was higher than that of the un-oxidized one, and it first increased with oxidation time, had the maximum value at 20 min, and then decreased. Such dependence of the density on the oxidation time was quite similar to that of the cycle life shown in Fig. 3.

The density of the specimen oxidized for 20 min was slightly higher than the theoretical density of Mg_2Ni, 3.46 $g \cdot cm^{-3}$. This discrepancy can be explained as follows. In the present case, the density of a sintered disk is determined not only by the sintering rate but also by the

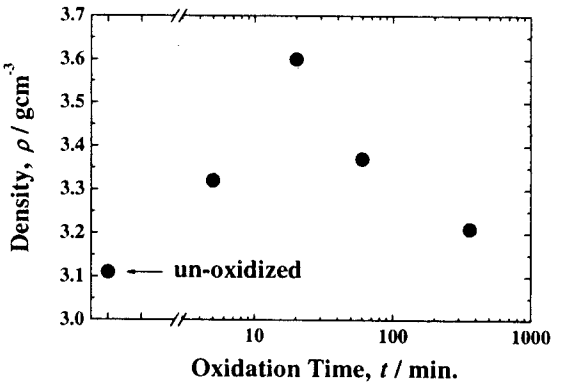

Fig. 5 Influence of pre-oxidation on density of sintered Mg_2Ni.

evaporation rate of magnesium. In our previous paper[6], it was reported that the magnesium concentration in the bulk of electrode after the sintering at 823 K was lower than the initial value by 6 mass%, and this was ascribed to the preferential evaporation of magnesium which took place during the sintering due to the low melting point of magnesium. Since the possible magnesium deficiency in Mg_2Ni structure is appreciably small[7], such preferential evaporation of magnesium should result in the formation of $MgNi_2$ and Ni phases. The densities of these phases are higher than that of Mg_2Ni, and hence the density of sintered disk can be higher than the theoretical density of Mg_2Ni.

The amount of evaporated magnesium during the sintering was estimated from the mass variation. The mass of the specimen oxidized for 20 min decreased to 96 % of the initial value during the sintering, while that of the un-oxidized specimen decreased to 94 %. This suggests that 9 and 13 % of magnesium evaporated for the former and the latter, respectively. Hence, the density of disk would be higher for the latter than for the former if the evaporation rate had dominant influence on the density. The density of the pre-oxidized specimens, however, was higher than that of the un-oxidized one. Hence, it is appropriate to consider that the influence of the sintering rate on the density is larger than that of the evaporation rate. For this reason, the result that the density of the pre-oxidized specimens was higher than that of the un-oxidized one indicates that the sintering rate increased with the pre-oxidation.

The dependence of the density on the oxidation time was quite similar to that of the cycle life as mentioned earlier. Therefore, it can be concluded that the cycle life increases with the sintering rate under the present experimental conditions. The mechanism behind this relationship between the sintering rate and the cycle life is discussed in 3.4.

3.3. Surface analysis

The results of surface analysis are summarized in table 1. The characteristic points of this table are the following:

(1) The concentration ratio of magnesium to nickel (Mg/Ni) was significantly higher than that in the bulk.

(2) Not only magnesium and nickel but also oxygen and carbon were observed.

(3) No significant change in the surface composition was brought about by the oxidation in air.

(4) The surface composition varied markedly with the heating in argon.

The concentration of carbon significantly decreased with the heating in argon, while no significant variation was observed in the concentration of oxygen. This suggests that the

Table 1 Surface compositions of Mg_2Ni sheets.

Treatment	Concentration (at%)			
	Mg	Ni	O	C
Polishing only	20	2	38	40
Oxidation in air	19	2	41	38
Oxidation in air plus heating in Ar	37	3	45	15
Heating in Ar	39	2	43	16

carbon was adsorbed onto the top surface of oxide film before the heating in argon and desorbed during the heating.

The spectra of Mg 2p, Ni $2p_{3/2}$ and oxygen 1s photoelectrons from the as-polished surface are shown in Fig. 6 (a). The peaks of Mg 2p and Ni $2p_{3/2}$ photoelectrons were observed at 51.1 and 855.7 eV, respectively. The binding energy of Ni $2p_{3/2}$ electrons is close to that in $Ni(OH)_2$ (855.6 eV) reported by McIntyre and Cook[8]. According to the literature[9], the binding energy of Mg 2p electrons of metallic magnesium (49.8 eV) shifts to 50.8 eV

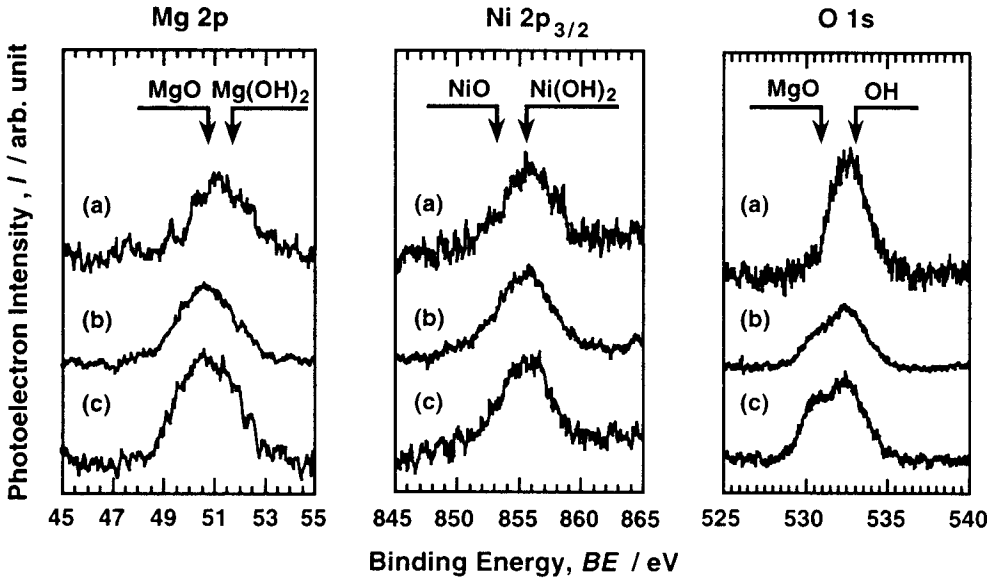

Fig. 6 Spectra of Mg 2p, Ni $2p_{2/3}$ and O 1s photoelectrons from (a) specimen in as-polished condition, (b) specimen oxidized in air and then heated in argon, (c) specimen heated in argon without pre-oxidation.

when magnesium is oxidized to MgO. The binding energy of Mg 2p electrons in Fig. 6 (a) is slightly higher than that corresponding to MgO. This can be ascribed to the coexistence of $Mg(OH)_2$ with MgO; it has been reported that the binding energy of Mg 2p electrons in $Mg(OH)_2$ is higher than that in MgO by 1 eV[10]. The peak of oxygen 1s spectrum was observed at 532.5 eV. According to Peng and Barteau[9] who examined the adsorption behavior of H_2O on a magnesium surface, the binding energy of oxygen 1s electrons in MgO is 531.0 eV and that in hydroxyl is 533.1 eV. The binding energy shown in Fig. 6 (a) is close to the latter. It seems appropriate to consider that the as-polished surface was covered with the thin MgO layer containing $Mg(OH)_2$ and $Ni(OH)_2$, and that the hydroxyls were adsorbed on the top surface of the oxide film. No significant change was observed in the spectra of Mg 2p, Ni $2p_{3/2}$ and oxygen 1s photoelectrons with the oxidation in air at 473 K.

The photoelectron spectra from the specimen heated in the argon atmosphere after the pre-oxidation in air are shown in Fig. 6 (b). The peak of Mg 2p spectrum was observed at 50.7 eV. This peak energy is slightly lower than that in Fig. 6 (a) and close to the binding energy of corresponding photoelectrons from MgO (50.8 eV). In oxygen 1s spectrum, a new peak was observed at 530.5 eV. This peak can be assigned to MgO. This indicates that the thickness of MgO layer increased during the heating through the reaction with oxygen present in the argon gas as an impurity.

In the case of the specimen heated in the argon atmosphere without the pre-oxidation in air, the peak energies of Mg 2p, Ni $2p_{3/2}$ and oxygen 1s photoelectrons were higher than those in Fig. 6 (b) by 1 eV. This can be attributed to electrostatic charging. Therefore, it is appropriate to consider that the thickness of the MgO layer was larger for this type of specimen than for the specimen with the pre-oxidation. The photoelectron spectra corrected for the charging are shown in Fig. 6 (c). In oxygen 1s photoelectron spectrum, the intensity of the peak corresponding to MgO (530.5 eV) is higher than that in Fig. 6 (b). This also indicates that the thickness of MgO layer on this type of specimen was larger than that on the specimen with the pre-oxidation. Therefore, it can be concluded that the growth rate of MgO layer during the heating in argon decreased with the pre-oxidation.

3.4. Mechanism underlying influence of pre-oxidation on discharge characteristics

The result that the cycle life increased with the sintering rate indicates that the bonding strength between the Mg_2Ni powder particles is one of important factors in determining the duration of cycle life under the present experimental conditions. The charge and the discharge bring about the volume expansion and reduction of the electrode,

respectively. In fact, the electrode was markedly deformed after the charge/discharge cycles. This cyclic variation of volume results in the initiation and the propagation of cracks which bring about the peeling of the Mg_2Ni particles. Therefore, the discharge capacity decreases with the propagation of the cracks. The initiation and the propagation rates of the cracks should decrease with increasing bonding strength between the particles. For this reason, the cycle life increased with the sintering rate.

The proposed mechanism that allows the improvement of cyclic stability with the pre-oxidation is as follows. During the sintering, the growth of MgO layer also took place as described in the previous section. The sintering rate should decrease markedly with increasing thickness of MgO layer since the melting point of MgO (3073 K) is significantly higher than the present sintering temperature (823 K) and hence the sintering of MgO does not take place under these conditions. The growth rate of MgO layer decreased with the pre-oxidation as mentioned above. Therefore, the sintering rate of the pre-oxidized powder was higher than that of the un-oxidized powder.

The reduction of the growth rate of MgO layer by the pre-oxidation can be explained as follows. According to Gregg and Jepson[11], oxide films formed on magnesium are coherent and protective below 723 K, and the breakdown of the oxide film takes place above this temperature. The molar volume of MgO is smaller than that of magnesium, and hence the

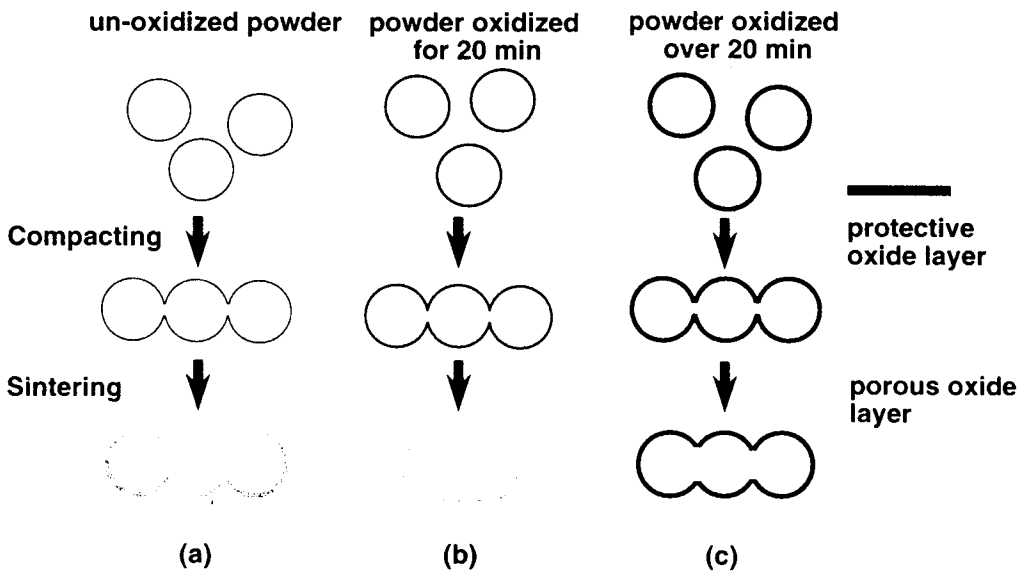

Fig. 7 Schematic description of mechanism underlying influence of pre-oxidation on sintering rate.

magnesium surface could not be completely covered by MgO. Therefore, they proposed that the oxide in the coherent film is in metastable phase a density of which is lower than that of stable MgO, and that the breakdown of the coherent film is caused by the recrystallization to the stable phase[11]. The precise nature of metastable phase, however, has not been clarified. It seems appropriate to consider that the surface of the Mg_2Ni powder used in the present study is covered by this coherent oxide film before the sintering. In the case of the powder without the pre-oxidation, this protective oxide layer would be thin as schematically shown in Fig. 7 (a). Hence, the breakdown of the protective oxide layer should take place easily, and the oxide layer should grow rapidly during the sintering. In the case of the pre-oxidized powder, the thickness of protective oxide layer should be large compared with the un-oxidized powder as shown in Fig.7 (b). Therefore, the oxide layer should keep on acting as the barrier to the further oxidation for longer time. For this reason, a mean growth rate of oxide layer during the sintering becomes smaller with the pre-oxidation. The cyclic stability was, however, degraded with the pre-oxidation over 20 min as shown in Fig. 3. This can be ascribed to the protective oxide layer becoming so thick as to act as the barrier to the sintering (see Fig.7 (c)).

The preferential oxidation of magnesium should result in the decrease of magnesium concentration in the alloy. Furthermore, the preferential evaporation of magnesium also takes place during the sintering as mentioned in 3.2. Therefore, $MgNi_2$ phase and nickel phase should appear at the oxide-alloy interface. The oxide films formed on these phases would be reduced easily during the charging process compared with the oxide film formed on the Mg_2Ni phase. This is because the free energy change for the formation of nickel oxide is far smaller than that of magnesium oxide. Therefore, $MgNi_2$ and nickel phases should act as the local reaction sites of hydrogen. The activation process observed in the initial stage of charge/discharge cycle should correspond to the reduction process of the oxide films formed on these phases.

The difference in the overpotential between the pre-oxidized specimen and the un-oxidized one shown in Fig. 4 cannot be attributed to the difference in the electrical resistance of the bulk of the specimens. This is because the density of the pre-oxidized specimen was higher than that of the un-oxidized specimen, and hence the resistance should be lower for the former than for the latter. The specific surface area of the pre-oxidized specimen would be smaller than that of the un-oxidized one since the sintering rate was higher for the former than for the latter. Therefore, the local current density would be higher for the pre-oxidized specimen than for the un-oxidized specimen. Such a difference in the local current density should be the reason why the overpotential is higher for the former than for the latter. The

surface area is, however, determined not only by the sintering rate but also by the evaporation rate of magnesium since the roughness of the powder surface should increase with the evaporation of magnesium. For this reason, this problem should be solved with the optimization of sintering conditions.

4. Conclusions

The influence of pre-oxidation on the discharge characteristics of sintered Mg_2Ni electrodes was examined. The results of the present study can be summarized as the following:

(1) The cyclic stability was improved markedly by the pre-oxidation. The maximum cycle life was obtained with the oxidation for 20 min.

(2) The density of sintered Mg_2Ni also increased with the pre-oxidation and had the maximum value with the oxidation for 20 min.

(3) The MgO layer was formed on the surface of Mg_2Ni during the sintering. The growth rate of the MgO layer decreased with the pre-oxidation.

(4) The improvement of cyclic stability with the pre-oxidation was attributed to the increase of sintering rate which results in the increase of bonding strength between the powder particles.

Acknowledgements

This work has been supported in part by a Grant-in-Aid for Scientific Research on Priority Areas A of "New Protium Function" of the Ministry of Education, Science, Sports and Culture. The authors are indebted for the gift of the cathode material to Human Environmental Systems Development Center of Matshushita Electric Industrial Co. and for that of the anode alloy powder to Japan Metals and Chemicals Co.

References

1) Y. Lei, Y. Wu, Q. Yang, J. Wu and Q. Wang, Z. Phys. Chem., Bd.183(1994)s.379

2) D. Sun, Y. Lei, W. Liu, J. Jiang, J. Wu and Q. Wang, J. Alloys and Compounds, 231(1995)621.

3) T. Kohno, S. Tsuruta and M. Kanda, J. Electrochem. Soc., 143(1996)L198.

4) T. Kohno and M. Kanda, J. Electrochem. Soc., 144(1997)2384

5) W. Liu, H. Wu, Y. Lei, Q. Wang, J. Wu, J. Alloys and Compounds, 252(1997)234.

6) W. M. Shu, K. Mizukami, K. Watanabe and S. Morozumi, Ann. Rept. of Hydrogen Isotope Res. Center, 17(1997)61.

7) T. B. Massalski, H. Okamoto, P. R. Subramanian and L. Kacprzak, "Binary Alloy Phase Diagrams", ASM International, OH, 1990.

8) N. S. McIntyre and M. G. Cook, Anal. Chem., 47(1975)2208.

9) X. D. Peng and M. A. Barteau, Surf. Sci., 233(1990)283.

10) P. Selvam, B. Viswanathan and V. Srinivasan, Int. J. Hydrogen Energy, 14(1989)899.

11) S. J. Gregg and W. B. Jepson, J. Inst. Metals, 87(1958)187.